machines

MDPI

Article

Design and Analysis of an Under-Actuated Adaptive Mechanical Gripper

Yulong Wei, Jiangtao Yu * and Ping Huo

School of Mechanical Engineering, North China University of Science and Technology, Tangshan 063210, China; yulong_weiyulong@163.com (Y.W.); huop@ncst.edu.cn (P.H.)
* Correspondence: yujt@ncst.edu.cn

Abstract

Robotic grippers play a crucial role in pick-and-place tasks, as their performance directly affects the robot's operational efficiency, stability, and safety. In industrial applications, such as coal gangue sorting, the target objects have irregular shapes and sharp surfaces, which pose challenges to the gripper's grasping ability. To solve these problems, an adaptive under-actuated gripper based on rope control is designed. The gripper is simple to control and combines the excellent features of both rigid and flexible grippers. To analyze the characteristics of the gripper, both mathematical analysis and holding force experiments are conducted. The results show that the gripper can generate a greater holding force when grasping larger objects with a constant input air pressure. Furthermore, irregularly shaped testing objects, including coal lumps and ores, are selected to conduct grasping experiments. The gripper achieves a 100% grasping success rate with a load of up to four times the object's weight suspended beneath it and shows the ability to reliably grasp irregularly shaped objects in high-speed pick-and-place tasks with a payload of four times the object's weight. Meanwhile, the gripper has a passive anti-collision ability due to the special outer contour of the distal finger when subjected to unexpected, sudden force.

Keywords: mechanical gripper; underactuated structure; adaptive grasping; cable-driven

1. Introduction

With the rapid advancement of intelligent manufacturing, industrial robots have become core equipment in automated production lines [1]. Industrial robots must exhibit diverse working characteristics to meet the varying demands of pick-and-place tasks. Grippers play a crucial role in fulfilling specific sorting requirements, and their performance directly affects the efficiency and suitability of the sorting process. In recent years, the demand for adaptive grippers that can handle irregular objects has grown significantly, driving continuous innovation in gripper design and control technologies [2].

This paper focuses on the design and application of adaptive rigid grippers for industrial sorting, specifically pick-and-place tasks, such as those encountered in coal gangue and ore sorting. The subject is an under-actuated, rope-controlled rigid gripper engineered for reliable and flexible grasping in such conditions. The proposed gripper achieves reliable grasping without complex control, making it suitable for pick-and-place environments where object sizes are inconsistent.

While various adaptive grippers have been developed for diverse fields [3–5], to the best of our knowledge, their deployment in pick-and-place tasks, such as coal gangue separation, remains limited. This application demands gripper adaptability to sharp objects,

Check for updates

Academic Editor: Guowu Wei

Received: 29 December 2025
Revised: 27 January 2026
Accepted: 30 January 2026
Published: 3 February 2026

Copyright: © 2026 by the authors. Licensee MDPI, Basel, Switzerland. This article is an open access article distributed under the terms and conditions of the Creative Commons Attribution (CC BY) license.

as well as rapid grasping and releasing. Soft and rigid–soft hybrid grippers, despite their excellent adaptability, often suffer from susceptibility to wear, tear, and material aging when handling sharp, irregular, and abrasive materials, leading to durability concerns. Therefore, there is a need for a gripper solution that combines the inherent robustness and high load capacity of rigid designs with the adaptive grasping ability necessary for irregular shapes, ensuring both reliability and efficiency.

The goal of this paper is to design, analyze, and validate a novel adaptive under-actuated gripper based on rope control, addressing the limitations of existing grippers. The proposed design aims to achieve a compact structure, flexible and shape-conforming grasping capability, and high reliability. Its potential contribution lies in providing a durable and effective gripper solution specifically tailored for pick-and-place tasks involving sharp and irregular objects in industries. Additionally, the proposed under-actuated design offers a method for balancing adaptability and durability, providing insights for future gripper development in similar fields.

The remainder of this paper is structured as follows: Section 2 reviews the state-of-the-art in gripper technology and identifies the research gap; Section 3 details the mechanical design, working principle, adaptive grasping ability, and passive anti-collision features of a cable-driven under-actuated rigid gripper; Section 4 presents the gripper's analytical model; Section 5 describes the simulation and experimental results; Section 6 discusses the key findings, contributions, performance comparisons with existing grippers, and limitations; Section 7 concludes with the main achievements and future work directions.

2. State of the Art

Existing grippers are primarily classified into rigid grippers, soft grippers, and rigid–soft hybrid grippers.

In the fields of industry and agriculture, rigid grippers are widely used in the sorting of objects. They feature a simple structure, high load capacity, and ease of control. Several scholars have conducted research on adaptive rigid grippers with multifunctional capabilities. Wu et al. [6] designed a novel asymmetrical under-actuated micro-gripper driven by a single piezoelectric actuator that can simultaneously realize the twisting and grasping operations of target objects. Kim et al. [7] proposed a compact gripper with an under-actuated mechanism and cable-driven actuation that enables stable grasping of objects with various shapes and sizes in unstructured environments. Liu et al. [8] proposed a self-adaptive rigid gripper that can adaptively grasp objects of various shapes and sizes by virtue of the elasticity of the connecting springs. Mouazé et al. [9] proposed an under-actuated gripper integrated with a bistable mechanism, specifically designed for grasping soft objects and suitable for applications such as food processing and medical applications. Wang et al. [10] proposed a passively adaptive five-fingered under-actuated dexterous hand that integrates the linkage-slider and rack—pinion mechanisms and features excellent dexterity, adaptability, and strong fingertip grasping capabilities. Park et al. [11] proposed an environmentally adaptive under-actuated gripper based on a cam mechanism. By virtue of the cam transmission structure, the gripper achieves an extended grasping stroke, while its fingertips perform linear motion, which mitigates collisions caused by positioning errors. Qiao et al. [12] developed an under-actuated gripper adopting tendon–pulley transmission and a two-stage linkage mechanism that achieves finger closure via a single-motor drive and is specifically designed for space debris removal. Kang et al. [13] designed a 3-DOF linkage-driven under-actuated gripper that is capable of achieving three operation modes, namely parallel grasping, shape-adaptive grasping, and environmental contact-based grasping. These grippers have been successfully applied in various fields, including food processing, agricultural harvesting, and underwater sampling.

https://doi.org/10.3390/machines14020175

To enhance the grasping of fragile objects, some researchers have investigated soft grippers with high adaptability and flexibility. Sofla et al. [14] developed a Fin Ray Effect (FRE)-based soft gripper that is specifically designed for the picking and placing of tree saplings in forest nurseries. Zhu et al. [15] designed a novel rope-driven force-sensing soft gripper based on the fin-shaped structure that can achieve the perception of contact nodes and contact forces without the need for additional sensors. Pagoli et al. [16] developed a novel dexterous soft gripper featuring a three-finger structure and an active palm that is capable of achieving human-like grasping functions. Inspired by octopus behaviors, Wu et al. [17] developed a 6-degrees-of-freedom multi-arm gripper. It can perform eight types of grasping motions. Guo et al. [18], Kodama et al. [19] and Li et al. [20] designed soft grippers by leveraging the characteristics of tendril plants. These grippers achieve adaptive grasping via winding and wrapping mechanisms. Phodapol et al. [21] proposed a viscous soft gripper inspired by insect tarsi. Some researchers have conducted designs based on Kirigami structures. Yang et al. [22] designed a soft gripper by combining a Kirigami structure and shape memory polymer (SMP). It achieves programmable deformation trajectories to fit object contours and realizes multi-mode grasping. Zhang et al. [23] proposed a pneumatic-cable-hybrid-driven gripper design based on origami finger structures that enables flexible adjustment of finger stiffness, length, and grasping range by regulating cable length and input air pressure. Chen et al. [24] proposed a variable-effective length (VEL) soft origami actuator based on tendon–pneumatic hybrid actuation, which can achieve the composite motion of elongation and bending. Kim et al. [25] designed a gripper with a double-layer stacked origami structure that is driven by fluid to achieve deployment and bending. Qi et al. [26] designed a Kirigami-based multi-stable flexible gripper that can flexibly switch between multiple configurations with only head segment actuation. The origami-based flexible gripper proposed by Liu et al. [27] can achieve cross-scale grasping from millimeters to decimeters via size scaling. To increase the load-carrying capacity of soft grippers, some researchers have proposed variable stiffness soft grippers. Li et al. [28] and Guo et al. [29] solved the problem of the insufficient load capacity of traditional soft grippers by adding a locking structure at the end of the flexible bending grippers. Zeng and Su [30] utilized layer jamming technology to adjust the stiffness of their gripper, ensuring adaptability to objects of complex shapes while achieving a stable loading of 6–10 kg. Sui et al. [31] proposed a soft fabric gripper featuring a simple structure, easy fabrication, low cost, and high load capacity. Ren et al. [32] implemented stiffness control in a gripper during grasping via granular jamming, and its maximum payload is equal to its own weight. Zhu et al. [33] proposed a variable-stiffness soft gripper based on rotational jamming layers to mitigate the interlayer slip phenomenon. Zhao and Wang [34] proposed a palm-shaped anthropomorphic variable-stiffness gripper that adopts 3D printed fabric jamming technology to achieve stiffness regulation. Huang et al. [35] proposed a morphology-configurable soft gripper assembled with self-adaptive modular composite fingers that is designed for soft grasping with high load capacity and self-sensing ability.

Some researchers have proposed rigid–flexible coupling grippers, which exhibit enhanced adaptability and reliability, thereby improving the load-carrying capacity of these grippers. For instance, the reconfigurable gripper based on three fingers proposed by Wang et al. [36] enables rapid switching between the rigid, rigid-bending, and flexible states. The reconfigurable dexterous gripper proposed by Wang et al. [37] enables switching between the rigid and flexible states. Based on a soft-enclosed grasping structure and a soft–rigid coupling structure, Li et al. [38] designed a high-load soft gripper capable of human body grasping, with the maximum payload increased to 90 kg and the maximum grasping size reaching 417 mm. Zhu et al. [39] designed a hybrid gripper with parallel coupling of a soft actuator (SA) and a rigid actuator (RA) that can selectively achieve the

high output force of an RA and the compliance of an SA, thus realizing high adaptability. The tendon-driven rigid–soft coupled robotic gripper proposed by Li et al. [40] exhibits excellent conformal grasping ability and strong perception capabilities for objects with minor dimensional variations. Kim et al. [41] developed a Linkage–Belt Hybrid (LBH) gripper specifically designed for plate pick-and-place robots. Trinh et al. [42] proposed a clamping device combining rigid fixtures and inflatable cushions that is suitable for object holding in vibrating environments. Wang et al. [43] developed a rigid–soft hybrid spherical shell gripper capable of stably grasping deformable, heavy, and irregularly shaped objects. Troisi et al. [44] and He et al. [45] proposed rigid–soft coupled grippers that achieve object grasping by maximizing the contact area between the gripper and the target object. Wang and Cheng [46] designed a rigid–soft coupled bionic gripper for casting pick-and-place robots that addresses the problem of insufficient adaptability in grippers for current small- and medium-sized casting pick-and-place robots.

However, in industrial sorting applications, such as coal gangue sorting and ore sorting, the shapes of objects are often irregular. Research on the application of adaptive rigid grippers in the coal gangue sorting process remains limited. The flexible components in soft and rigid–flexible coupling grippers are susceptible to wear and aging in such environments, significantly compromising their durability.

To solve these problems, an adaptive underactuated gripper based on a cable-driven mechanism is designed. By employing a pneumatic cylinder for actuation, torsion springs for self-resetting, and flexible cables for force transmission, the gripper achieves a combination of rigid construction and adaptability. This design enables stable and reliable grasping of sharp and irregularly shaped objects, making it suitable for pick-and-place tasks involving sharp and irregularly shaped objects.

3. Mechanical Design

The overall structure of the robot gripper is illustrated in Figure 1, and it consists of a driving unit and two symmetrically arranged, independently actuated clamping units. The driving unit consists of a driven cylinder, pulley 1, rope 1, a sliding component, and pulley 2. Pulley 1 is mounted on the driven cylinder, while pulley 2 is mounted on the end of the sliding component. Both ends of rope 1 are attached to the top of the sliding component. The clamping unit consists of rope 2, the proximal finger, the distal finger, shaft 1, shaft 2, and shaft 3. The proximal finger rotates about shaft 1 and features a limiting structure that contacts the base. In the absence of external forces, it remains in an extended position under the action of torsion spring 1. The distal finger rotates around shaft 2, while shaft 3 is attached to the proximal finger. The distal finger features a limiting structure that contacts shaft 3. In the absence of external forces, it remains in an extended position under the action of torsion spring 2. Both ends of rope 2 are attached to shaft 3, and the attachment points are on shaft 3.

When the cylinder extends, the taut rope 1 moves upward along with pulley 1, driving the sliding component and pulley 2 to move upward. Then, the taut rope 2 forces the proximal finger to rotate around shaft 1. Due to torsion spring 2 and the limiting structure, the angle between the proximal finger and the distal finger remains unchanged, so the distal finger moves correspondingly. Ultimately, the distal fingers make contact with the object. Thus, the gripper achieves a closed state and completes the grasping action.

This gripper possesses the ability to automatically adapt to the shape of an object. When grasping an irregular object, one of the clamping units will first reach a holding position, rendering its pulley 2 fixed. Pulley 2 of the other clamping unit continues to move upward, driven by the cylinder, until all distal fingers make contact with and fully hold the

irregular object. It allows each distal finger to independently find its stable position against the object's surface.

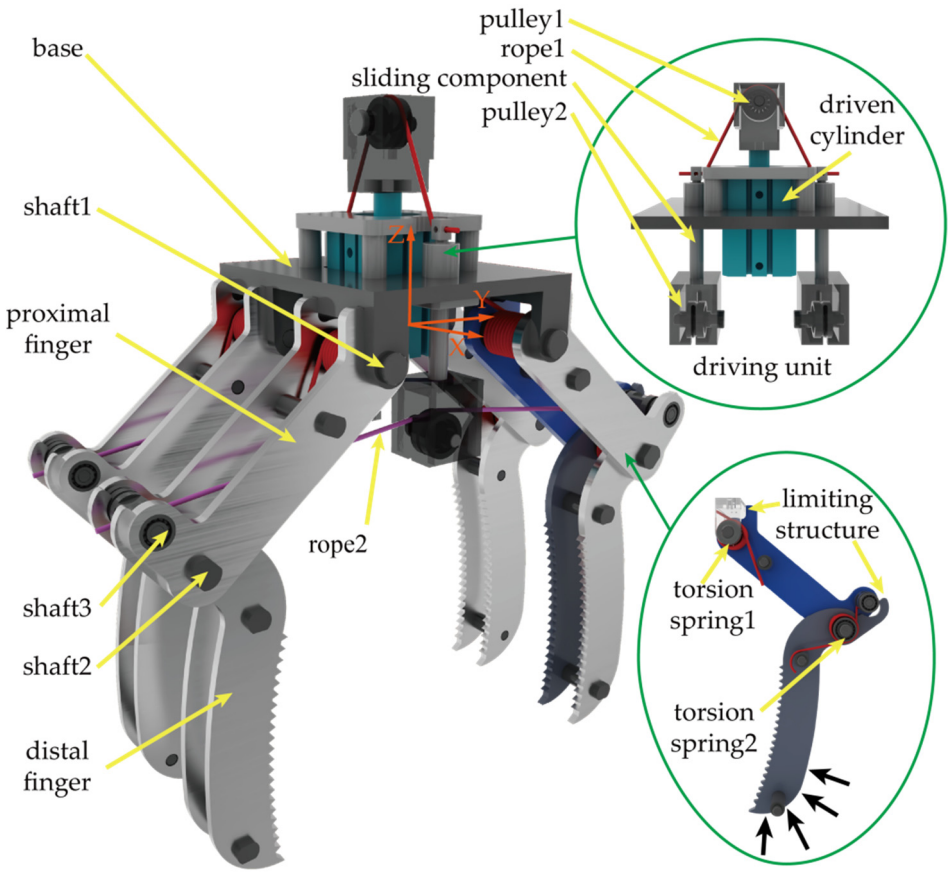


Figure 1. Overall structure of the gripper.

The gripper has a passive anti-collision ability. The outer contour of the distal finger features a specially designed curvature. When subjected to external force, the component of the external force acting in the normal direction of the designed curvature generates a torque that overcomes the torsion of torsion spring 2, causing the distal finger to rotate inward, as shown in Figure 1. The inward rotational movement of the distal finger is permitted, which prevents damage to the gripper itself from unexpected collision.

In addition, this gripper is easy to control. It only requires one digital output point in the control system to control its solenoid valve. When the solenoid valve is energized to extend the cylinder, the two clamping units on both sides move inward, finishing the picking operation. When the solenoid valve is de-energized to retract the cylinder, the gripper opens, completing the placement operation.

For the subsequent analysis of the mechanism, a coordinate system is established, as shown in Figure 1. The *X*-axis is perpendicular to the plane of the clamping unit, the *Y*-axis is parallel to the clamping unit plane, and the *Z*-axis aligns with the cylinder axis. The coordinate origin is located on the horizontal plane that contains the axis of rotating shaft 1.

4. Analytical Model

4.1. Analysis of the Driving Unit

The schematic diagram of the driving unit is shown in Figure 2.

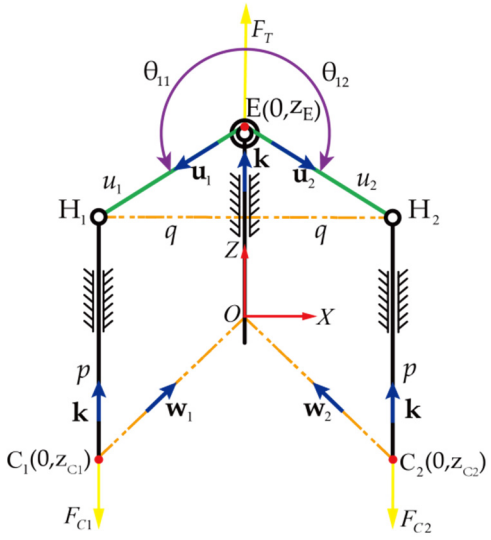


Figure 2. Schematic diagram of the driving unit.

To simplify the calculation, the following hypotheses are assumed. Rope 1 contacts the highest point of pulley 1, denoted as point E. The fixed connection points between rope 2 and the two sliding components are denoted as point H_n, treated as rotation pairs. Rope 2 contacts the highest point of pulley 2, denoted as point C_n.

$2q$ denotes the horizontal distance between H_1 and H_2, p denotes the length of rod H_nC_n, and u_n denotes the two portions of rope 1 with length l_{r1}, which denotes the length of rope segment H_nE. Vectors $\mathbf{u}_n$, $\mathbf{w}_n$, and $\mathbf{k}$ denote the unit vectors along the directions of EH_n, C_nO and the z-axis respectively. z_E and z_{C_n} denote the z-coordinates of points E and C_n respectively.

For the closed-loop OEH_nC_n, the vector equation can be expressed as

$$\mathbf{w}_n + z_E\mathbf{k} + u_n\mathbf{u}_n = p\mathbf{k} \tag{1}$$

Based on Equation (1), the following relationship between z_E and z_{C_n} can be acquired.

$$z_E = z_{C_1} - k_1 l_{r1}\cos\theta_{11} + p = z_{C_2} - (1 - k_1) l_{r1}\cos\theta_{12} + p \tag{2}$$

where

$$\theta_{11} = \pi - \arcsin\left(\frac{q}{k_1 l_{r1}}\right) \tag{3}$$

$$\theta_{12} = \pi - \arcsin\left(\frac{q}{(1-k_1) l_{r1}}\right) \tag{4}$$

$$k_1 = \begin{cases} \frac{1}{2} - \frac{1}{2}\sqrt{1 - \frac{\left(l_{r1}^2 - \Delta C^2\right)^2 + 4\Delta C^2 q^2}{l_{r1}^2\left(l_{r1}^2 - \Delta C^2\right)}} & , \ \Delta C \le 0 \\ \frac{1}{2} + \frac{1}{2}\sqrt{1 - \frac{\left(l_{r1}^2 - \Delta C^2\right)^2 + 4\Delta C^2 q^2}{l_{r1}^2\left(l_{r1}^2 - \Delta C^2\right)}} & , \ \Delta C > 0 \end{cases} \tag{5}$$

$$\Delta C = z_{C_2} - z_{C_1} \tag{6}$$

Neglecting gravity and friction, a force analysis of the driving unit yields the following equation.

$$F_{C_n} = \frac{F_T \cos\theta_{1n}}{\cos\theta_{11} + \cos\theta_{12}} \tag{7}$$

where F_T is the cylinder force acting on rope 1, and F_{C_n} is the rope 2 force acting on pulley 2.

4.2. Analysis of the Clamping Unit

A schematic diagram of the clamping unit is shown in Figure 3.

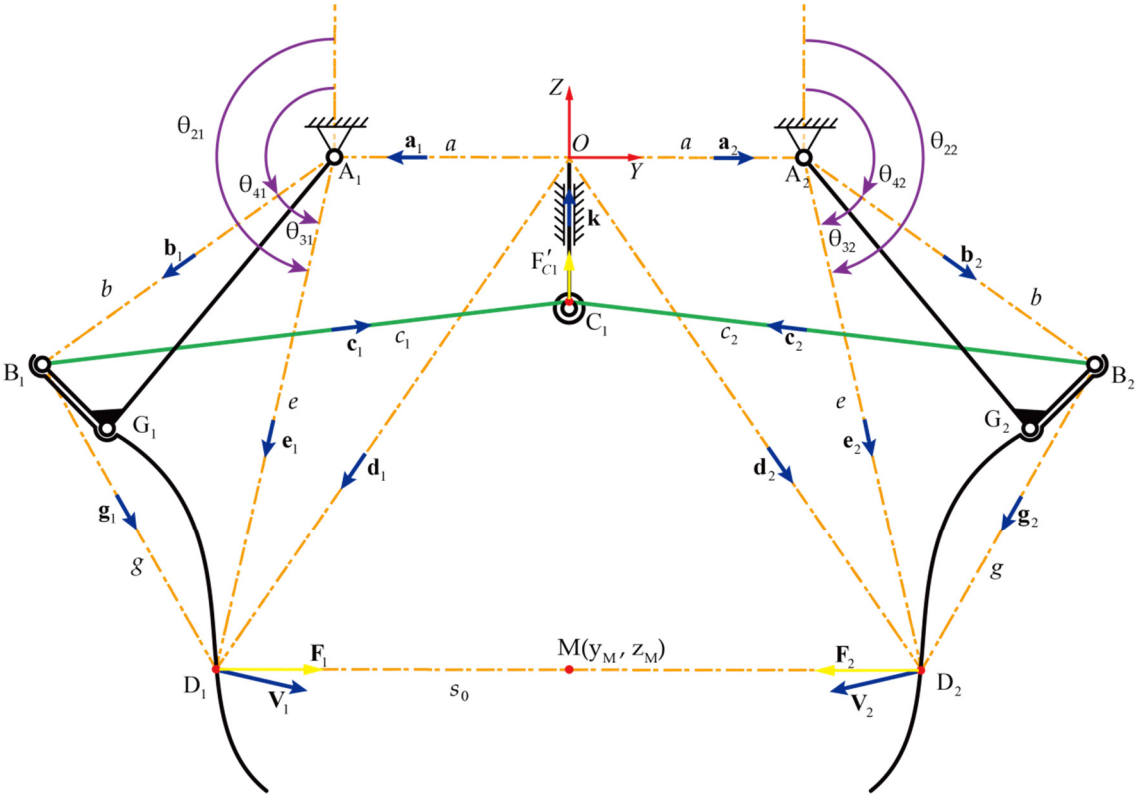


Figure 3. Schematic diagram of the clamping unit.

Points A, G, and B denote the accumulation points of the axis lines of shaft 1, shaft 2 and shaft 3 respectively. D_i is assumed to be the contact points between the gripper and the object, with their midpoint being M.

a, b, e, and g denote the length of rods OA_i, A_iB_i, A_iD_i, and B_iD_i respectively. s_0 and y_M denote the distance of D_1D_2 and the y-coordinate of point M respectively. c_i represents the two portions of rope 2 with length l_{r2}, which denotes the length of cable segment B_iC_1. Vectors $\mathbf{a}_i$, $\mathbf{b}_i$, $\mathbf{c}_i$, $\mathbf{d}_i$, $\mathbf{e}_i$, and $\mathbf{g}_i$ denote the unit vector along the directions of OA_i, A_iB_i, B_iC_1, OD_i, A_iD_i, and B_iD_i respectively. Vector $\mathbf{v}_i$ denotes the velocity of the contact point, $\mathbf{d}_i$. The output point, C_1, of the drive unit is the input of one clamping unit. F'_{C_1} and F_{C_1} are interaction forces.

$$\mathbf{b}_i = \mathbf{\Lambda}_{1i} \times \mathbf{k} \tag{8}$$

$$\mathbf{e}_i = \mathbf{\Lambda}_{2i} \times \mathbf{k} \tag{9}$$

where

$$\mathbf{\Lambda}_{1i} = \cos\theta_{2i} + \sin\theta_{2i}\mathbf{k} \tag{10}$$

$$\mathbf{\Lambda}_{2i} = \cos\theta_{4i} + \sin\theta_{4i}\mathbf{k} \tag{11}$$

For the closed-loop OA_iD_i and $OA_iB_iC_1$, the vector equation can be expressed as

$$\mathbf{d}_i = a\mathbf{a}_i + e\mathbf{e}_i \tag{12}$$

$$-z_{C_1}\mathbf{k} + a\mathbf{a}_i + b\mathbf{b}_i + c_i\mathbf{c}_i = 0 \tag{13}$$

Based on Equations (12) and (13), the following relationship between s_0, y_M, and z_{C_1} can be acquired.

$$\sqrt{z_{C_1}^2 + M - z_{C_1} N \cos\theta_{41} + Q\sin\theta_{41}} + \sqrt{z_{C_1}^2 + M - z_{C_1} N \cos\theta_{42} + Q\sin\theta_{42}} = k_2 l_{r2} \quad (14)$$

where

$$M = a^2 + b^2 \quad (15)$$

$$N = 2b \quad (16)$$

$$Q = 2ab \quad (17)$$

$$\theta_{4i} = \mathrm{sgn}(i)\arccos\left(\frac{\frac{s_0}{2} - \mathrm{sgn}(i) y_M - a}{e}\right) + \mathrm{sgn}(i)\frac{\pi}{2} - \theta_{3i} \quad (18)$$

$$\theta_{3i} = \mathrm{sgn}(i)\arccos\left(\frac{b^2 + e^2 - g^2}{2be}\right) \quad (19)$$

$$\mathrm{sgn}(i) = \begin{cases} 1 & , i = 1 \\ -1 & , i = 2 \end{cases} \quad (20)$$

Due to the multi-toothed design of the gripper's distal finger, two primary contact modes, i.e., tooth embedding and point contact, can occur when grasping irregular objects, as shown in Figure 4. For tooth embedding, the normal force acting on the embedded surface plays a key role in grasping. However, for point contact, friction is the decisive factor. Therefore, an ideal mathematical model analysis is complex. Under stable grasping conditions, the horizontal components of the clamping forces (HCCFs) provided by the two distal fingers are equal in magnitude and opposite in direction, which is a critical factor influencing both the tooth embedding effect and the point contact effect. A larger HCCF strengthens the effect in tooth embedding and increases friction in point contact. At larger bending angles, when the multi-tooth structure contacts the object, the normal direction of the contact surface approaches the vertical direction. For the same horizontal clamping force, the normal force on the embedded surface increases, enhancing the gripping stability of the gripper.

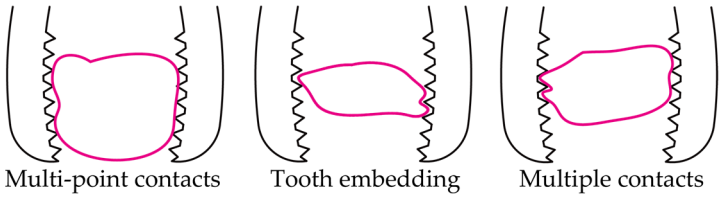


Figure 4. Various contact modes.

Therefore, the subsequent analytical modeling will neglect the gravity and friction of each finger and assume that the clamping force acts along the horizontal direction; the clamping force can be acquired based on the principle of virtual work.

$$\mathbf{F}'_{C_1} \cdot \Delta z_{C_1} = \sum_{i=1}^{2} (\mathbf{F}_i \cdot \Delta \mathbf{d}_i + k_N \theta_{5i} \Delta\theta_{4i}) \quad (21)$$

where $\mathbf{F}'_{C_1}$ is the pulley 2 force acting on rope 2, $\mathbf{F}_i$ is the gripper clamping force, k_N is the torsional spring 1 stiffness, and θ_{5i} is the current angle of torsional spring 1.

For Equation (21), the following relationship between s_0; y_M; F'_{C_1}, the norm of $\mathbf{F}'_{C_1}$; and F_i, the norm of $\mathbf{F}_i$, can be acquired.

$$F_1 = F_2 = \frac{F'_{C_1}\frac{P_1+P_2\frac{\cos\theta_{42}}{\cos\theta_{41}}}{P_4} - P_3}{P_5} \tag{22}$$

where

$$P_1 = \frac{-z_{C_1}N\sin\theta_{41} - Q\cos\theta_{41}}{R_1} \tag{23}$$

$$P_2 = \frac{-z_{C_1}N\sin\theta_{42} - Q\cos\theta_{42}}{R_2} \tag{24}$$

$$R_1 = \sqrt{z_{C_1}^2 + M - z_{C_1}N\cos\theta_{41} - Q\sin\theta_{41}} \tag{25}$$

$$R_2 = \sqrt{z_{C_1}^2 + M - z_{C_1}N\cos\theta_{42} - Q\sin\theta_{42}} \tag{26}$$

$$P_3 = k_N\left(\theta_{51} + \theta_{52}\frac{\cos\theta_{42}}{\cos\theta_{41}}\right) \tag{27}$$

$$P_4 = \frac{2z_{C_1} - N\cos\theta_{41}}{R_1} + \frac{2z_{C_1} - N\cos\theta_{42}}{R_2} \tag{28}$$

$$P_5 = -e\cos\theta_{21} - e\cos\theta_{22}\frac{\cos\theta_{42}}{\cos\theta_{41}} \tag{29}$$

5. Experiment and Results

5.1. Simulating Calculation

To evaluate the clamping force, the two clamping units are both assumed to be in a symmetrical state. The clamping force, varying with input air pressure and clamping width, is calculated using MATLAB R2024a. The main structural parameters of the gripper are listed in Table 1.

Table 1. Main structural parameters.

Parameters	Value
l_{r1} (mm)	125.42
l_{r2} (mm)	270.52
p (mm)	74
q (mm)	36
a (mm)	42
b (mm)	102.84
e (mm)	208.05
g (mm)	162.56
k_N (N·mm/deg)	15.024

The relationship between air pressure, clamping width, and clamping force is shown in Figure 5a. Analysis of Figure 5b shows that when the clamping width remains constant, the higher the air pressure, the greater the clamping force. Analysis of Figure 5c shows that when the air pressure is constant, the larger the clamping width, the greater the clamping force. This proves the application potential of the gripper in holding large objects.

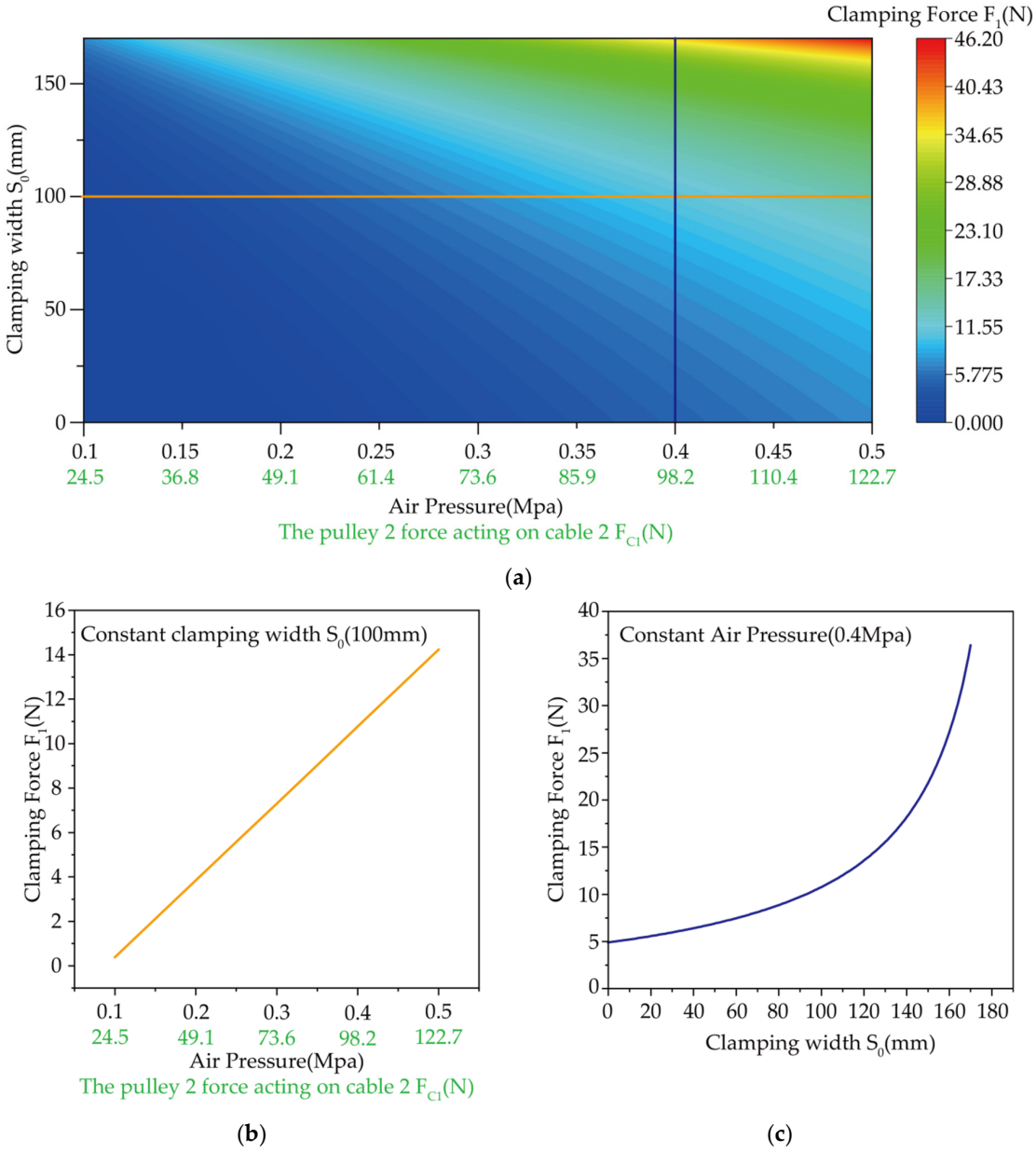


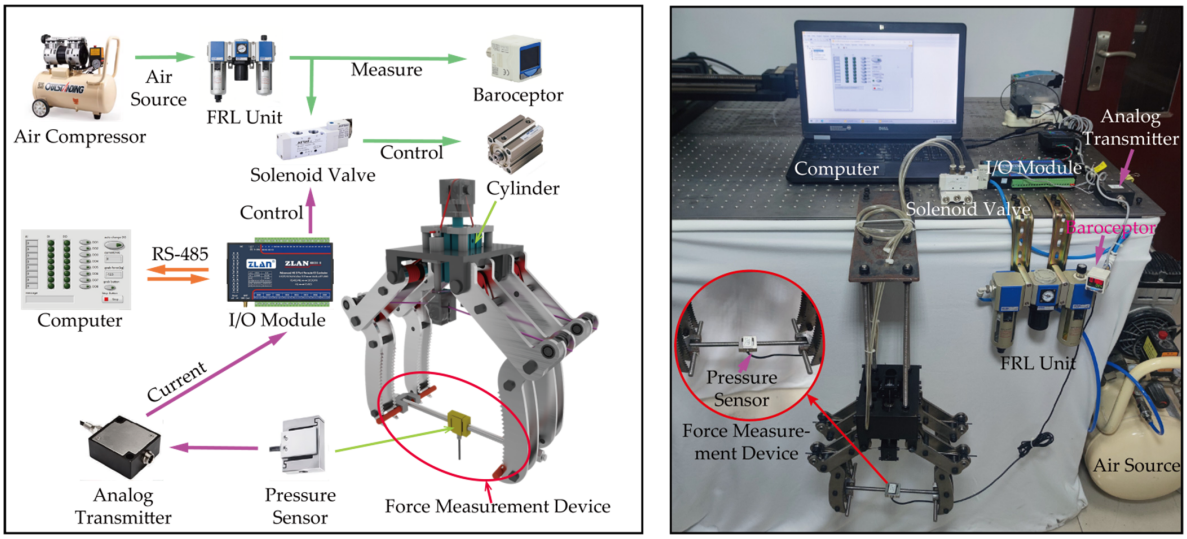
Figure 5. (**a**) Relationship between air pressure, clamping width, and clamping force; (**b**) constant clamping width; (**c**) constant air pressure.

5.2. Clamping Force Measurement Experiment

To verify the gripper's performance, an experimental platform was constructed, as shown in Figure 6, and a force measurement device was designed to measure the clamping force. The IO module, communicating with the computer program, controls the solenoid valve to actuate the cylinder's extension and retraction while automatically collecting clamping force data from the pressure sensor mounted on the force measurement device. To observe the input air pressure, a baroceptor is installed in the pneumatic circuit.

Pneumatic System Components: Air compressor (OTS-1500), Outstanding, Taizhou, China; FRL unit (GR300-08), Airtac, Taiwan, China; Solenoid valve (5V-110-06), Airtac, Taiwan, China; Cylinder (CQSB25-30D), Airtac, Taiwan, China; and Baroceptor (DPSN1), Airtac, Taiwan, China. Electrical Control and Measurement Components: Pressure sensor (JLBS-M2-50kg), Zhongnuo, Bengbu, China; Analog transmitter (BSQ-3), Zhongnuo, Bengbu, China; I/O module (ZLAN-6808-1), ZLAN, Shanghai, China; and Computer (Dell Precision 3510), DELL, State of Texas, America.

The primary structure of the gripper mechanism was manufactured from low-carbon steel (Q235) due to its low cost and favorable machinability, which satisfies the functional requirements of the gripper. To enhance the durability of the distal finger, it is manufactured from titanium alloy, which offers high hardness and wear resistance. The rope is a high-strength steel wire rope, providing the necessary tensile strength and flexibility for force transmission.



(**a**) (**b**)

Figure 6. (**a**) Experimental platform composition; (**b**) photograph of the physical platform.

During the experiment, the distance of the force measurement device is set to be 50 mm, 125 mm, 150 mm, 163 mm, and 170 mm to simulate grasped objects of different sizes. Different air pressures were regulated using an FRL (Filter–Regulator–Lubricator) unit. The clamping force is measured with different object sizes and air pressures. Each point value is the average of data from five tests, which constitute the error bar. As shown in Figure 7, the theoretical calculations are presented simultaneously, which are consistent with the experimental data.

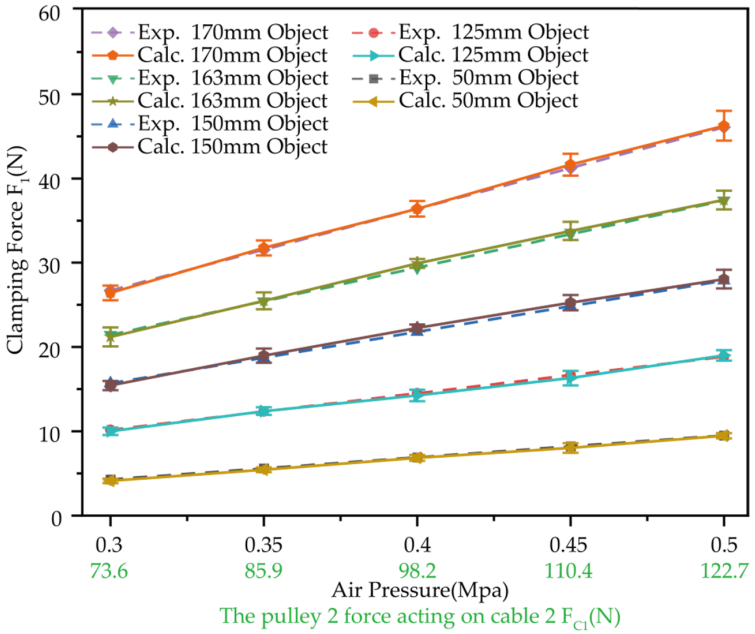


Figure 7. Experimental results of clamping force.

5.3. Physical-Object-Holding Experiment and Discussion

To evaluate the gripper's practical performance, a physical-object-holding experiment was conducted, as illustrated in Figure 8. During the experiment, irregularly shaped objects, such as coal blocks and ores, were grasped under an air pressure of 0.5 MPa, progressively increasing the suspended weight until grasping failure occurred.

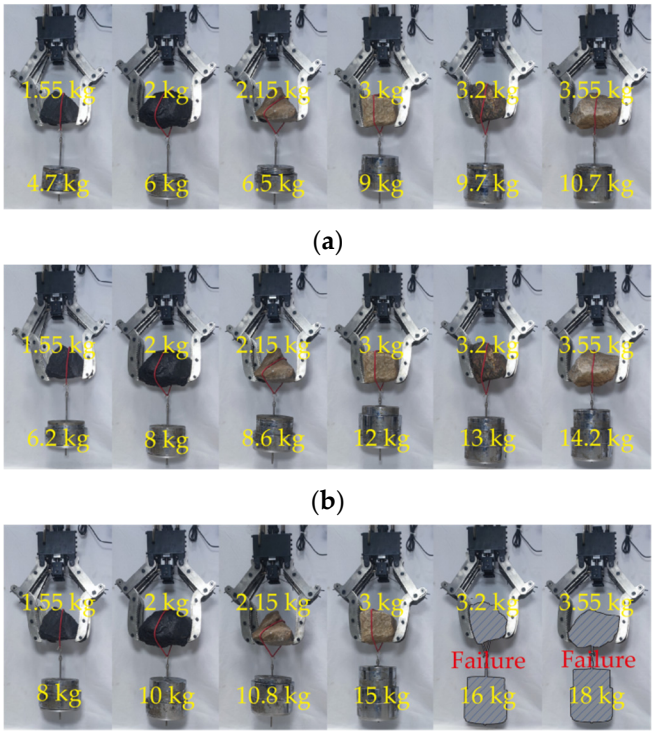


Figure 8. (**a**) Suspending three times the weight of the object; (**b**) suspending four times the weight of the object; (**c**) suspending five times the weight of the object.

Each object was grasped ten times at each load level. In the experiments, the gripper demonstrated a 100% success rate under load conditions of three and four times the object's weight, demonstrating reliable clamping stability and a payload capacity of up to four times the object's weight. However, grasping failures occurred at a load level of five times the object's weight.

In addition, the gripper was successfully applied to a coal gangue pick-and-place application, as shown in Video S1. This gripper can sort coal gangue of different shapes and sizes, significantly improving operational efficiency.

6. Discussion

The primary contribution of this work is the successful development and validation of a cable-driven, rigid, under-actuated gripper specifically designed for handling irregular, sharp, and abrasive objects, such as coal gangue and ores. The gripper successfully combines high-load-capacity rigid designs with adaptive grasping capabilities through an under-actuated, cable-driven design. Under a constant air pressure input, the gripper generates a greater holding force when grasping larger objects. This property is particularly advantageous for securely holding irregular lumps of varying sizes. Physical grasping experiments confirm that the gripper can reliably hold irregular objects with a suspended load of at least four times the object's weight. Furthermore, it demonstrates stable operation in high-speed pick-and-place tasks under accelerations up to 4 g. Due to the specially

contoured outer surface, upon unexpected impact, the force component normal to this contour induces an inward rotation of the finger, mitigating potential damage to the gripper or the object.

Meanwhile, a comparison is conducted between the experimental results of this work and the state-of-the-art grasping technologies reviewed in Section 2. The comparison focuses on payload-to-weight ratio, maximum grasping range, and actuation method. These indicators directly reflect the gripper's load-bearing capacity, adaptability to object size, and operational complexity. Detailed comparison data are summarized in Table 2.

Table 2. Comparison with grippers in Section 2.

Reference	Type	Payload-to-Weight Ratio	Maximum Grasping Range	Actuation
Liu et al. [8]	Rigid	0.6	6~380 mm	One Electric Motor
Kang et al. [13]	Rigid	2.1	0~260 mm	Three Electric Motors
Zhu et al. [15]	Flexible	2.53	8~100 mm	One Electric Motor and Pneumatic Drive
Zeng et al. [30]	Flexible	21.1	100~150 mm	0.5 Mpa Pneumatic Drive
Li et al. [38]	Rigid–flexible	4.7	0~417 mm	0.4 Mpa Pneumatic Drive
He et al. [45]	Rigid–flexible	1.95	63~86 mm	One Electric Motor
This article	Rigid	3.55	0~170 mm	0.5 Mpa Pneumatic Drive

As shown in Table 2, some rigid grippers adopt an electric motor drive and lead screw transmission, which exhibit poor dynamic response characteristics in the grasping or release period. Although flexible and rigid–flexible grippers possess adaptability, their flexible materials are prone to wear when in contact with sharp coal gangue. In contrast, the rigid gripper designed in this paper is driven by an air cylinder. It not only achieves adaptive grasping but also has the ability to handle sharp objects and enables fast actuation, making it more suitable for the engineering requirements of efficient coal gangue sorting.

Although the gripper demonstrated reliable grasping with suspended loads of up to four times the object's weight, grasping failures occurred at the five-times load condition. This indicates a practical upper limit to its load-bearing capability under the tested configuration. Furthermore, the multi-toothed design of the gripper's distal finger enhances the stability of clamping. When the distal finger wears out, it reduces the gripper's clamping ability. In practical applications, it is used as a quick-wear component. However, the distal finger is a plate-type component that is easy to manufacture. In the future, efforts will be focused on improving the gripper to make it more stable when dealing with more complex situations.

7. Conclusions

In conclusion, a cable-driven under-actuated gripper is proposed, driven by only one air cylinder, that features a simple structure and ease of control. Designed with pulleys, torsion springs, and steel cables, the gripper possesses a stable holding ability for irregularly shaped objects due to each distal finger being in the clamping state synchronously. Designed with a special outer contour on its distal finger, the gripper possesses a self-protection ability from sudden collisions due to each distal finger being able to rotate inward under external force. Greater air pressure and larger grasped objects, along with the more clamping force, endow the gripper with the ability to adapt to differently sized objects under high-speed conditions with a payload four times that of the object's weight.

Compared with traditional rigid grippers and flexible grippers, this gripper possesses the characteristics of high load capacity and shape adaptiveness, which gives it considerable potential in industrial applications of reliable pick-and-place operations. Future work will

focus on improving the grasping capability for irregular objects to better address high-speed application scenarios.

Supplementary Materials: The following supporting information can be downloaded at https://www.mdpi.com/article/10.3390/machines14020175/s1: Video S1: A coal gangue pick-and-place application.

Author Contributions: Methodology, J.Y. and Y.W.; formal analysis, Y.W.; investigation, Y.W.; writing—original draft preparation, Y.W.; writing—review and editing, J.Y. and P.H.; supervision, J.Y. and P.H.; project administration, J.Y. All authors have read and agreed to the published version of the manuscript.

Funding: This research was funded by the Major Scientific and Technological Achievements Transformation Project, grant number 23284001Z, supported by the State-owned Assets Supervision and Administration Commission of the People's Government of Hebei Province.

Data Availability Statement: The original contributions presented in this study are included in the article. Further inquiries can be directed to the corresponding author.

Conflicts of Interest: The authors declare no conflicts of interest.

References

1. Chen, H.; Zhu, J.; Cao, Y.; Xia, Z.; Chai, Z.; Ding, H.; Wu, Z. Soft-rigid coupling grippers: Collaboration strategies and integrated fabrication methods. *Sci. China Technol. Sci.* **2023**, *66*, 3051–3069. [CrossRef]
2. Sun, Y.; Liu, Y.; Pancheri, F.; Larg, T.C. A lightweight robotic gripper with 3-d topology optimized adaptive fingers. *IEEE/ASME Trans. Mechatron.* **2022**, *27*, 2026–2034. [CrossRef]
3. Ahmed, F.; Waqas, M.; Jawed, B.; Soomro, A.M.; Kumar, S.; Hina, A.; Khan, U.; Kim, K.H.; Choi, K.H. Decade of bio-inspired soft robots: A review. *Smart Mater. Struct.* **2022**, *31*, 073002. [CrossRef]
4. Chen, X.; Zhang, X.; Huang, Y.; Cao, L.; Liu, J. A review of soft manipulator research, applications, and opportunities. *J. Field Robot.* **2022**, *39*, 281–311. [CrossRef]
5. Ji, H.; Lan, Y.; Nie, S.; Huo, L.; Yin, F.; Hong, R. Development of an anthropomorphic soft manipulator with rigid-flexible coupling for underwater adaptive grasping. *Soft Robot.* **2023**, *10*, 1070–1082. [CrossRef] [PubMed]
6. Wu, Z.; Wang, Y.; Chen, M.; Ding, B. Design, analysis, and experimental investigations of an asymmetrical under-actuated micro-gripper. *J. Intell. Mater. Syst. Struct.* **2024**, *35*, 960–970. [CrossRef]
7. Kim, M.; Yoon, J.; Kim, D.; Yun, D. Development of a Hybrid Gripper with Jamming Module Using Small-scale Pneumatic Pump. *Int. J. Control. Autom. Syst.* **2024**, *22*, 3341–3351. [CrossRef]
8. Liu, C.; Cheng, J.; Li, Z.; Cheng, C.; Zhang, C.; Zhang, Y.; Zhong, R.Y. Design of a self-adaptive gripper with rigid fingers for Industrial Internet. *Robot. Comput. Integr. Manuf.* **2020**, *65*, 101976.101971–101976.101979. [CrossRef]
9. Mouazé, N.; Birglen, L. Bistable compliant underactuated gripper for the gentle grasp of soft objects. *Mech. Mach. Theory* **2022**, *170*, 104676. [CrossRef]
10. Wang, D.; Xiong, Y.; Zi, B.; Xian, S.; Zhu, W.D. Design, analysis and experiment of a passively adaptive underactuated robotic hand with linkage-slider and rack-pinion mechanisms. *Mech. Mach. Theory* **2020**, *155*, 104092. [CrossRef]
11. Park, S.J.; Jeon, H.J.; Meng, J.H.; Song, J.B. Gripper with Adaptability to Environmental Constraints. *IEEE Robot. Autom. Lett.* **2024**, *9*, 6608–6615. [CrossRef]
12. Qiao, S.L.; Liu, R.Q.; Guo, H.W.; Liu, Y.X.; Deng, Z.Q. Configuration Design of an Under-Actuated Robotic Hand Based on Maximum Grasping Space. *Chin. J. Mech. Eng.* **2018**, *31*, 35. [CrossRef]
13. Kang, L.; Kim, S.-H.; Yi, B.-J. Modeling, design, and implementation of an underactuated gripper with capability of grasping thin objects. *Machines* **2021**, *9*, 347. [CrossRef]
14. Sofla, M.S.; Golshanian, H.; Sklar, E.I.; Calisti, M. Development of a soft gripper for replicating human grasps in forest nursery tasks. *Robot. Auton. Syst.* **2025**, *189*, 104987. [CrossRef]
15. Zhu, Z.; Liu, Y.; Ju, J.; Lu, E. Design and Experimental Test of Rope-Driven Force Sensing Flexible Gripper. *Sensors* **2024**, *24*, 6407. [CrossRef]
16. Pagoli, A.; Chapelle, F.; Corrales, J.A.; Mezouar, Y.; Lapusta, Y. A soft robotic gripper with an active palm and reconfigurable fingers for fully dexterous in-hand manipulation. *IEEE Robot. Autom. Lett.* **2021**, *6*, 7706–7713. [CrossRef]
17. Wu, M.; Afridi, W.H.; Wu, J.; Afridi, R.H.; Wang, K.; Zheng, X.; Wang, C.; Xie, G. Octopus-inspired underwater soft robotic gripper with crawling and swimming capabilities. *Research* **2024**, *7*, 0456. [CrossRef]

18. Guo, X.; Tang, W.; Qin, K.; Zhong, Y.; Xu, H.; Qu, Y.; Li, Z.; Sheng, Q.; Gao, Y.; Yang, H. Powerful UAV manipulation via bioinspired self-adaptive soft self-contained gripper. *Sci. Adv.* **2024**, *10*, eadn6642. [CrossRef]
19. Kodama, H.; Ide, T.; Yunhao, F.; Nabae, H.; Suzumori, K. Vine-Like, Power Soft Gripper Based on Euler's Belt Theory. *IEEE Robot. Autom. Lett.* **2024**, *9*, 3108–3115. [CrossRef]
20. Li, L.; He, S.; Qi, Q.; Zeng, J.; Kang, S.; Endo, G.; Nabae, H.; Ma, S.; Suzumori, K. Pegrip: A plant-tendril-inspired passive entanglement gripper enabling fail-safe grasping. *IEEE Robot. Autom. Lett.* **2024**, *9*, 7039–7046. [CrossRef]
21. Phodapol, S.; Harnkhamen, A.; Asawalertsak, N.; Gorb, S.N.; Manoonpong, P. Insect tarsus-inspired compliant robotic gripper with soft adhesive pads for versatile and stable object grasping. *IEEE Robot. Autom. Lett.* **2023**, *8*, 2486–2493. [CrossRef]
22. Yang, Y.; Wang, P.; Liu, J.; Fu, Y.; Shen, Y. Tunable stiffness Kirigami gripper based on shape memory polymer and supercoiled polymer artificial muscle for multi-mode grasping. *Smart Mater. Struct.* **2024**, *33*, 14. [CrossRef]
23. Zhang, Z.; Fan, W.; Long, Y.; Dai, J.; Luo, J.; Tang, S.; Lu, Q.; Wang, X.; Wang, H.; Chen, G. Hybrid-Driven Origami Gripper with Variable Stiffness and Finger Length. *Cyborg Bionic Syst.* **2024**, *5*, 0103. [CrossRef] [PubMed]
24. Chen, B.; Shao, Z.; Xie, Z.; Liu, J.; Pan, F.; He, L.; Zhang, L.; Zhang, Y.; Ling, X.; Peng, F.; et al. Soft Origami Gripper with Variable Effective Length. *Adv. Intell. Syst.* **2021**, *3*, 2000251. [CrossRef]
25. Kim, W.; Eom, J.; Cho, K.-J. A dual-origami design that enables the quasisequential deployment and bending motion of soft robots and grippers. *Adv. Intell. Syst.* **2022**, *4*, 2100176. [CrossRef]
26. Qi, Z.; Sun, X.; Xu, J. A Kirigami Multi-Stable Flexible Gripper with Energy-Free Configurations Switching. *Adv. Intell. Syst.* **2024**, *6*, 2400038. [CrossRef]
27. Liu, J.; Chen, Z.; Wen, G.; He, J.; Wang, H.; Xue, L.; Long, K.; Xie, Y.M. Origami Chomper-Based Flexible Gripper with Superior Gripping Performances. *Adv. Intell. Syst.* **2023**, *5*, 10. [CrossRef]
28. Li, H.; Zhou, P.; Zhang, S.; Yao, J.; Zhao, Y. A high-load bioinspired soft gripper with force booster fingers. *Mech. Mach. Theory* **2022**, *177*, 105048. [CrossRef]
29. Guo, X.-Y.; Li, W.-B.; Gao, Q.-H.; Yan, H.; Fei, Y.-Q.; Zhang, W.-M. Self-locking mechanism for variable stiffness rigid-soft gripper. *Smart Mater. Struct.* **2020**, *29*, 035033. [CrossRef]
30. Zeng, X.; Su, H. A High Performance Pneumatically Actuated Soft Gripper Based on Layer Jamming. *J. Mech. Robot.* **2023**, *15*, 014501. [CrossRef]
31. Sui, D.; Wang, T.; Zhao, S.; Zhang, X.; Zhao, J.; Zhu, Y. An Enveloping Soft Gripper with High-Load Carrying Capacity: Design, Characterization and Application. *IEEE Robot. Autom. Lett.* **2022**, *7*, 373–380. [CrossRef]
32. Ren, T.; Li, Y.; Liu, Q.; Chen, Y.; Yang, S.X.; Yuan, H.; Li, Y.; Yang, Y. Novel bionic soft robotic hand with dexterous deformation and reliable grasping. *IEEE Trans. Instrum. Meas.* **2023**, *72*, 1–10. [CrossRef]
33. Zhu, M.; Xie, M.; Yue, K.X. A Variable Stiffness Soft Gripper Based on Rotational Layer Jamming. *Soft Robot.* **2024**, *11*, 85–94. [CrossRef]
34. Zhao, Y.; Wang, Y. A palm-shape variable-stiffness gripper based on 3D-printed fabric jamming. *IEEE Robot. Autom. Lett.* **2023**, *8*, 3238–3245. [CrossRef]
35. Huang, H.; Tang, S.; Chai, W.; Sun, F.; Wu, D.e.; Miao, S.; Zhong, D.; Hou, H.; Dong, M. MCSG: A morphology configurable soft gripper with self-adaption modular composite finger. *IEEE Trans. Ind. Electron.* **2023**, *71*, 708–717. [CrossRef]
36. Wang, H.; Gao, B.; Hu, A.; Xu, W.; Shen, H.; He, J. Design of a Reconfigurable Gripper with Rigid-Flexible Variable Fingers. *IEEE/ASME Trans. Mechatron.* **2025**, *30*, 505–516. [CrossRef]
37. Wang, H.; Gao, B.; Hu, A.; He, J. A Variable Stiffness Gripper with Reconfigurable Finger Joint for Versatile Manipulations. *Soft Robot.* **2023**, *10*, 1041–1054. [CrossRef]
38. Li, H.; Zhang, S.; Zhang, X.H.; Zhao, W.M.; Yao, J.T. A 0.5-meter-scale, high-load, soft-enclosed gripper capable of grasping the human body. *Sci. China Technol. Sci.* **2023**, *66*, 501–511. [CrossRef]
39. Zhu, J.; Chai, Z.; Yong, H.; Xu, Y.; Guo, C.; Ding, H.; Wu, Z. Bioinspired Multimodal Multipose Hybrid Fingers for Wide-Range Force, Compliant, and Stable Grasping. *Soft Robot.* **2023**, *10*, 30–39. [CrossRef]
40. Li, Z.; Yin, M.; Huang, B.; Cai, Z.; Yi, Z.; Wu, X. A spring-based rigid-soft robotic gripper for conformal grasping and object recognition. *J. Braz. Soc. Mech. Sci. Eng.* **2024**, *46*, 249. [CrossRef]
41. Kim, Y.H.; Shin, J.P.; Won, J.; Lee, W.; Seo, T.W. LBH gripper: Linkage-belt based hybrid adaptive gripper design for dish collecting robots. *Robot. Auton. Syst.* **2025**, *185*, 104886. [CrossRef]
42. Trinh, H.X.; Nguyen, H.-H.; Pham, T.-D.; My, C.A. A novel rigid-soft gripper for safe and reliable object handling. *J. Braz. Soc. Mech. Sci. Eng.* **2024**, *46*, 176. [CrossRef]
43. Wang, Z.; Kanegae, R.; Hirai, S. Circular Shell Gripper for Handling Food Products. *Soft Robot.* **2021**, *8*, 542–554. [CrossRef] [PubMed]
44. Troisi, D.; Dragusanu, M.; Pozzi, M.; Prattichizzo, D.; Malvezzi, M. A Soft-Rigid Gripper for Safe Handling and Transportation. *Adv. Mater. Technol.* **2025**, *10*, 2401592. [CrossRef]

45. He, Z.; Lian, B.; Song, Y. Rigid-Soft Coupled Robotic Gripper for Adaptable Grasping. *J. Bionic Eng.* **2023**, *20*, 2601–2618. [CrossRef]
46. Wang, C.J.; Cheng, B. Design of a robotic gripper for casting sorting robots with rigid–flexible coupling structures. *Robotica* **2024**, *42*, 2658–2676. [CrossRef]

Disclaimer/Publisher's Note: The statements, opinions and data contained in all publications are solely those of the individual author(s) and contributor(s) and not of MDPI and/or the editor(s). MDPI and/or the editor(s) disclaim responsibility for any injury to people or property resulting from any ideas, methods, instructions or products referred to in the content.